Testing of Adaptive Beamsteering for Interference Rejection in GNSS Receivers

David S. De Lorenzo, Stanford University
Felix Antreich, German Aerospace Center (DLR)
Holmer Denks, German Aerospace Center (DLR)
Achim Hornbostel, German Aerospace Center (DLR)
Christian Weber, German Aerospace Center (DLR)
Per Enge, Stanford University

BIOGRAPHY

David De Lorenzo is a member of the Stanford University GPS Laboratory, where he is pursuing a Ph.D. degree in Aeronautics and Astronautics. He received a Master of Science degree in Mechanical Engineering from the University of California, Davis, in 1996. David has worked previously for Lockheed Martin and for the Intel Corporation.

Felix Antreich received the Dipl. -Ing. degree in Electrical Engineering from Munich University of Technology (TUM) in 2003. Since July 2003 he is with the Institute for Communications and Navigation of the German Aerospace Center (DLR). He is Ph.D. candidate at the TUM. He is Member of IEEE.

Holmer Denks received his Engineer Diploma in Electric Engineering and Communications at the University of Kiel, Germany, in 2002. He was involved in investigation and simulation of communications systems. In 2002 he joined DLR. Currently he works on simulations of Galileo signals.

Achim Hornbostel joined the German Aerospace Center (DLR) in 1989 after he had received his Engineer Diploma in Electrical Engineering at the University of Hannover in the same year. In 1995 he received the PhD in Electrical Engineering from the University of Hannover. In 2000 he became member of staff at the Institute of Communications and Navigation at DLR, where he is now leading a working group for receivers and algorithms since 2005. He was involved in several projects for remote sensing, satellite communications and satellite navigation. His main activities are currently in signal propagation and receiver development.

Christian Weber graduated from Technical University of Munich in 2004. He worked at Fraunhofer-Gesellschaft as a research fellow in the field of communication systems. Since 2005 he is with the German Aerospace Center (DLR) focusing on interference effects on GNSS receivers. He is leading the interference activities for safety of life applications in the Institute of Communications and Navigation of DLR. He is a member of VDE/ITG and IEEE.

Dr. Per Enge is a Professor of Aeronautics and Astronautics at Stanford University, where he is the Kleiner-Perkins, Mayfield, Sequoia Capital Professor in the School of Engineering. He directs the GPS Research Laboratory, which develops satellite navigation systems based on the Global Positioning System. Dr. Enge has received the Kepler, Thurlow, and Burka Awards from the Institute of Navigation for his work. He is a Fellow of the Institute of Navigation and the Institute of Electrical and Electronics Engineers.

ABSTRACT

In this work space-time adaptive processing algorithms for interference rejection in a GNSS receiver are tested under experimental conditions with recorded signals generated by a powerful hardware signal generator. Two space-time adaptive processing algorithms are tested which are implemented in the Stanford University GPS multi-antenna space-time adaptive software receiver. The Multi-output Advanced Signal Test Environment for Receivers (MASTER) developed by Spirent and DLR is used for signal generation and the NordNav-R30 Quad Frontend is used for recording.

INTRODUCTION

The precision provided by current generation GNSS (Global Navigation Satellite System) receivers, together with the use of sophisticated processing methods such as differential and kinematic techniques, leaves interference and multipath as dominant remaining error sources affecting GNSS performance. In the worst case, a GNSS receiver encountering strong interference or multipath might not be able to track a sufficient number of satellite signals to obtain a navigation solution. However, even if the navigation solution is available, the pseudorange and/or carrier-phase accuracy may be degraded, raising continuity and integrity issues especially for safety-critical applications.

Thus, a receiver that is not prepared to detect and mitigate undesired in-band signals either will lose lock of valuable satellites or will let the navigation solution be degraded without notification to the user. Multi-element adaptive antenna arrays and other spatial and temporal filtering techniques have attracted substantial interest in recent years for their ability to increase incoming signal-to-noise ratio, as well as to reject interference and/or multipath, e.g., [1, 2, 3, 4, 5, 6].

The work described in this paper covers three main areas: 1) a multi-antenna signal simulator, 2) an adaptive beamsteering GNSS software receiver, and 3) the RFI (radio frequency interference) performance of several space-time adaptive algorithms, using as a metric the tracked C/No.

A satellite signal simulator system, the Multi-output Advanced Signal Test Environment for Receivers (MASTER), developed by Spirent and DLR [7], generates up to 48 digital I/Q-baseband signals corresponding to 48 individual GPS or Galileo satellites, signal multipath and interference. These baseband signals are digitally weighted and combined by an external digital processing device in order to map the individual signals to the elements of an array antenna by considering the phase shifts due to the spatial distribution of the antenna elements (i.e., wavefront generation). After weighting and summing, the digital signals are fed back to the simulator for digital to analog conversion, mixing to a common intermediate frequency, and then final up-conversion to the carrier. The resultant signals, each representing one antenna element with all available satellites with RFI included, are recorded by a NordNav-R30 Quad Frontend. The recorded signals then are fed as inputs into a software-based all-in-view GNSS receiver developed by the GPS Laboratory at Stanford University [1]. Distinguishing this receiver implementation is the inclusion of array-processing modules, either for deterministic beamsteering or for adaptive beamsteering and nullforming using space-time adaptive processing.

In this work, deterministic beamsteering, adaptive beamsteering, and nullforming using space-time adaptive processing are assessed in order to effectively reject radio frequency interference (RFI) in a GNSS receiver. Adaptation that seeks to minimize the mean-squared error between the arriving signal and a locally-generated reference signal is able to reject RFI significantly better than a deterministic beamformer, even without first solving for the arrival vector of the RFI signals. Adaptation that uses explicit knowledge of the direction-of-arrival of the desirable signal performs comparably to the deterministic beamformer in the interference-free case, but suffers in RFI rejection due to analog hardware issues and scenario parameters that were identified in the course of this investigation. In general, the methods investigated and described in this work represent a practical approach to adaptive beamsteering/nullforming GNSS receiver design for efficient RFI mitigation.

SOFTWARE RECEIVER OVERVIEW

This section presents an overview of the Stanford University GNSS multi-antenna space-time adaptive software receiver [1], shown in Figure 1. The basic processing of the receiver follows traditional design practices. An FFT-based acquisition module performs a rapid search across Doppler frequency and code-phase for satellite signals present in the input data. For GPS signals, up to ten milliseconds of coherent integration during acquisition is normally allowed. Following acquisition, normal GNSS signal processing takes place: carrier wipeoff, code wipeoff, early/prompt/late inphase and quadrature correlators, and then execution of code and carrier tracking loops. The desired characterization data for this investigation are present in the code-phase, carrier-phase, and carrier to noise ratio (C/N_0) estimates. For this reason, computation of a navigation solution is not required.

The non-standard feature of this software receiver is the inclusion of a weight control algorithm which supports single-antenna FRPA (fixed reception pattern antenna), multi-antenna deterministic CRPA (controlled reception pattern antenna), and space-time adaptive antenna array processing. The execution of the adaptive weight control algorithm can occur between the carrier and code wipeoff steps as shown in Figure 1, or it can occur downstream of the correlation operation.

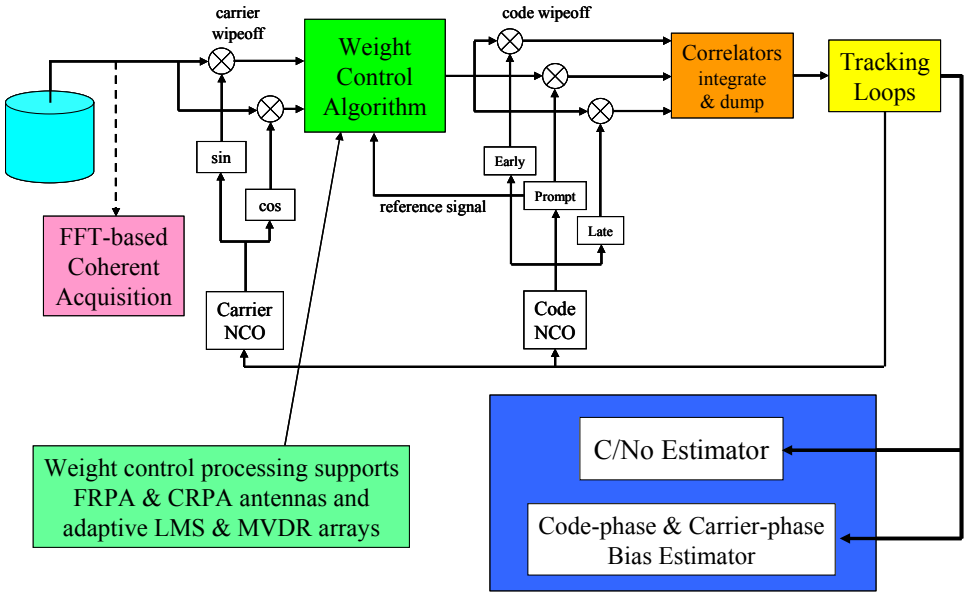

Figure 1. Software receiver block diagram.

SPACE-TIME ADAPTIVE ANTENNA ARRAY PROCESSING

This section describes the approach to adaptive processing for GPS. There is a substantial history of adaptive signal processing and STAP for radar systems and wireless communication [8, 9, 10, 11], with the primary goals being to reject interference, to increase the signal to noise ratio (SNR), and to reduce the bit-error-rate of transmitted data. Current GPS methods build on this existing technology base. For GPS, there is an additional critical goal of limiting timing errors (or equivalently, limiting delays) in the code-phase and carrier-phase estimates. A unique constraint for GPS is that the signals tracked by the receiver are below the thermal noise floor before code de-spreading. This characteristic makes reference-signal-based adaptation more challenging and has led much of the previous research to focus strictly on power minimization methods.

The central concept of an adaptive antenna array is the use of feedback to optimize some performance index (see Figure 2 and Compton, 1988 [12]). "Adaptive" in this context means that the array gain pattern adapts to the signal and noise environment, subject to user-specified constraints. The constraint or optimization criteria can be broadly classified as either maximizing the signal to interference plus noise ratio (SINR) at the array output, e.g., [13, 14], or minimizing the mean-squared error (MSE) between the actual array output and the ideal array output, e.g., [15]. In both cases, the array adapts to maximize the desired signal and to reject interference.

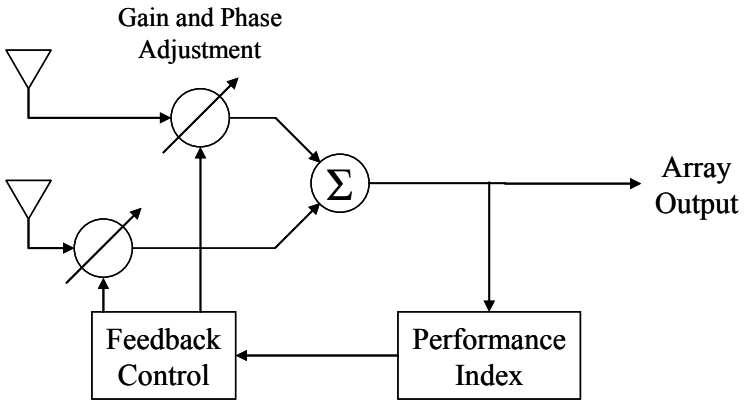

Figure 2. Generic adaptive antenna array (after Compton, 1988).

For the purposes of this investigation, two adaptation schemes are studied. The Applebaum beamformer [14], or minimum variance distortionless response (MVDR) array, is in the SINR-class of methods. This algorithm constrains to unity the array gain in a particular look direction (it also may have side constraints for nullsteering), while rejecting coherent interference down to the noise floor. The Widrow beamformer [15] is in the MSE-class of methods. This algorithm seeks a weight vector that causes the array output to match a desired reference signal, while again rejecting coherent interference present at the array input. This is termed a least-mean-squared (LMS) approach as it uses an LMS-based error cost function.

The Widrow/LMS and Applebaum/MVDR optimization criteria were chosen for the following reasons: (a) they are the prototypical examples of each class of adaptive weight control method mentioned above, (b) these methods are ones against which other adaptive schemes typically are compared, (c) they are straightforward to implement and relatively efficient to execute, (d) they are well-represented in the radar, wireless, and GPS literature, and (e) they have well-understood convergence properties and stability can be guaranteed with an appropriate choice of adaptation parameters.

In both cases the optimal steady-state weight vectors satisfy the Wiener solution:

$$\begin{aligned} \mathbf{W}_{MVDR} &= \mu\boldsymbol{\Phi}^{-1}\mathbf{T}^* \quad Applebaum/MVDR \\ \mathbf{W}_{LMS} &= \boldsymbol{\Phi}^{-1}\mathbf{S} \quad Widrow/LMS \end{aligned} \tag{1}$$

This notation, and that used henceforth in this investigation, comes from Compton, 1988 [12]. Here **T*** is the array steering vector, **S** is the reference correlation vector, and **Φ** is the signal covariance matrix, which is defined as the expected value of $\mathbf{X}^*\mathbf{X}^T$ (**X** being the measurement vector). In the interference-free case, the signal covariance matrix **Φ** is diagonal and the weight vector **W** is equal to the constraint vector scaled according to the gain of each antenna.

Note that solution of the equations in this form requires estimation and then inversion of **Φ**. This is the sample matrix inverse (SMI) approach. Estimation of **Φ** can require significant signal buffering capacity (placing large memory demands on the receiver) and time-averaging (introducing latency and reducing the ability of the array to adapt quickly to changing signal environments), while matrix inversion requires computational complexity. However, this is an approach that has been employed successfully in adaptive beamforming and nullsteering GPS architectures, e.g., [16, 17, 18].

In recursive form, these adaptive algorithms look like:

$$\begin{aligned} \mathbf{W}_{n+1} &= \left[\mathbf{I} - \gamma\boldsymbol{\Phi}_n\right]\mathbf{W}_n + \gamma\mu\mathbf{T}^* \quad Applebaum/MVDR \\ \mathbf{W}_{n+1} &= \left[\mathbf{I} - \gamma\boldsymbol{\Phi}_n\right]\mathbf{W}_n + \gamma\mathbf{S}_n \quad Widrow/LMS \end{aligned} \tag{2}$$

With this formulation, estimation of **Φ** is not tied to SMI buffer size, but may be done at each sample epoch. Thus, solving for the weight vector subject to the adaptive constraints requires no buffering or matrix inversion, and with suitable pre-conditioning adapts quickly to a changing signal environment.

As update equations, the algorithms become:

$$\begin{aligned} \Delta\mathbf{W}_n &= \gamma\left[\mu\mathbf{T}^* - \boldsymbol{\Phi}_n\mathbf{W}_n\right] \quad Applebaum/MVDR \\ \Delta\mathbf{W}_n &= \gamma\left[\ \mathbf{S}_n - \boldsymbol{\Phi}_n\mathbf{W}_n\right] \quad Widrow/LMS \\ \mathbf{W}_{n+1} &= \mathbf{W}_n + \Delta\mathbf{W}_n \end{aligned} \tag{3}$$

This last form is actually the most instructive. The algorithms reach steady-state when the bracketed terms in the $\Delta\mathbf{W}_n$ equations are zero, i.e., when the weight vector suppresses from the covariance matrix everything but the steering or reference vector. Of course, since only an estimate of the covariance matrix, **Φ**, is available, this is an approximate solution. It is the misadjustment parameter γ (equivalent to 2μ in the treatment of Widrow and Stearns, 1985 [19]) that controls convergence speed and, as the name implies, steady-state misadjustment.

The Applebaum/MVDR array is well-suited to situations of known signal arrival direction and known antenna response, but unknown signal waveform. In fact, MVDR array performance is negatively impacted by channel errors, line biases, or unmodeled antenna effects. If **T*** includes nullsteering constraints, then the MVDR array also is sensitive to interference localization errors. In contrast, the Widrow/LMS array is appropriate for unknown signal arrival direction but known (or correlated) reference waveform. While the LMS array is

resistant to the error sources just mentioned for the MVDR array, it may be susceptible to multipath-induced biases, since the LMS cost function will steer array sidelobes to capture multipath energy. The MVDR array will not suffer this effect.

ARRAY PROCESSING IN A GPS RECEIVER

In a GPS receiver, code wipeoff follows carrier wipeoff, and uses the estimated code-phase from the code numerically-controlled oscillator (NCO). This is followed by accumulation:

$$S = \frac{1}{T}\sum_{t=1}^{T} s(t)\cdot x(t-\hat{\tau}) \tag{4}$$

Eq. 4 is executed for the prompt code replica, as well as for early and late code replicas. The accumulator outputs are used in the code-phase and carrier-phase discriminators, which drive the code and carrier tracking loops.

For a multi-antenna GPS receiver, weight vector multiplication can occur either pre-correlation or post-correlation. In pre-correlation beamforming, the antenna weights are applied to the antenna signals directly (after carrier wipeoff). In post-correlation beamforming, the antenna weights are applied after the complex correlation operation. Since both accumulation and beamforming are linear operations, they can be done in either order:

$$\begin{aligned} S &= \frac{1}{T}\sum_{t=1}^{T}\left(\sum_{j=1}^{N} s_j(t)\cdot w_j\right)\cdot x(t-\hat{\tau}) \qquad pre-correlation \\ &= \frac{1}{T}\sum_{j=1}^{N}\left(\sum_{t=1}^{T} s_j(t)\cdot x(t-\hat{\tau})\right)\cdot w_j \qquad post-correlation \end{aligned} \tag{5}$$

Eq. 5 expands the signal vector, $s(t)$, and shows that weight vector multiplication and code wipeoff and accumulation are order-independent. (This discussion does not cover beamforming that occurs outside of the main receiver processing flow, e.g., beamforming as a separate stand-alone anti-jam module or STAP appliqué.) Note that pre-correlation beamforming occurs at the sampling frequency (~MHz speeds) while post-correlation beamforming occurs at the integrate-and-dump frequency (~kHz).

MULTI-OUTPUT ADVANCED SIGNAL TEST ENVIRONMENT FOR RECEIVERS (MASTER)

The general measurement setup consists of DLR's Multi-output Advanced Signal Test Environment for Receivers (MASTER), which includes the signal generator boxes, the control PC and the up-converters on one side, and the device under test (normally a GNSS receiver) on the other. A data recording unit could replace the receiver. Optional parts of MASTER are the wavefront matrix and a vector signal generator. A schematic

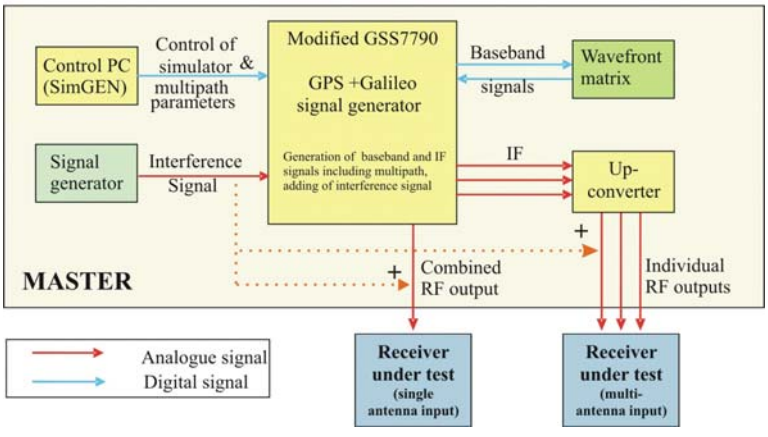

Figure 3. Schematic overview of MASTER.

Figure 4. DLR MASTER.

overview of the system is given by Figure 3. A picture of MASTER is shown in Figure 4.

The core of MASTER consists of two modified GSS7790 multi-output full constellation simulators by Spirent which provide all GPS (L1, L2, L5) and Galileo (E1, E5, E6) satellite signals as digital baseband signals. One important feature of MASTER is the availability of these baseband signals via an LVDS interface which enables a manipulation of the satellite signals by a digital processing matrix called MATRIX developed by DLR. The manipulation can be represented by a complex multiplication of the GNSS I/Q signals provided by the simulator with complex coefficients. Coefficients can change at a rate up to 100 Hz. One application of the MATRIX is to account for the phase shift of the signal with respect to the spatial distribution of the antenna elements of a multi-element patch antenna array. For details of the baseband wavefront generation with the MATRIX see [7].

MASTER is controlled by the software application SimGEN® running on a control PC. SimGEN® enables the user to define a simulation environment including parameters such as orbit parameters of the GNSS satellites, clock errors, iono- and tropospheric effects, antenna pattern, multipath, and user trajectories. It also is used to define the satellite signal and its components, such as navigation data, pilot/data channel, and modulation scheme according to the desired frequency band. On that same PC typically the coefficients for the MATRIX are generated in a pre-run of the simulation and then sent to the MATRIX via USB during the simulation.

For the desired satellite signals two different signal paths are available, either all signals combined on one output or each signal individually. In the first case the signal generated in baseband and possibly manipulated by the MATRIX is mixed to a common IF for all GPS and Galileo frequency bands, put on the appropriate carrier and finally filtered. It is available on the combined output at a nominal power level of about -130 dBm and a dynamic range of ±20 dB. This signal can directly be fed into a single antenna GNSS receiver. The second case is much more powerful. The signals are each individually available on individual IF ports. They are then routed by BNC cables to the desired RF up-converter to be mixed to RF. Finally the signals are available on the individual RF outputs representing either one satellite signal or, in the case of a multi-antenna receiver simulation, all satellite signals corresponding to one antenna element. The power of the GNSS signals at these ports is approximately 40 dB higher than at the combined output. Note that the allocation of the signals to specific hardware channels, in addition to the phase shifting, is done by using the appropriate coefficients within the MATRIX [7].

An important feature of MASTER is the possibility to provide GNSS signals overlaid with other signals, i.e. interferers, in the same frequency band. There are two different ways of providing the user with interfering signals. The first way is to generate these signals within the modified GSS7790 simulator boxes. This enables the user to manipulate the interferers in the same way as the desired satellite signals. The signals then are processed in the same way as the GNSS signals and can be tapped at the appropriate RF outputs. The drawback of this method is the limited maximal power of the signals at the RF output of up to -60 dBm. Besides this limitation, the types of interferers are limited to continuous wave (CW), broadband interferers, or GNSS like signals. The second way of generating interference overcomes these limitations. In this method, a powerful programmable signal generator (Agilent PSG E8267D) is used instead. With this signal generator, signals can be generated almost arbitrarily. The drawback here is that phase shifted copies of a signal for multiple antenna outputs have to be created at RF-level, which is not foreseen with the current measurement set-up. An alternative, which is a subject for future work, is to generate or to record digital I/Q baseband interference signals and feed them into one input of the matrix at the appropriate sampling rate together with the I/Q satellite baseband signals at the other inputs of the MATRIX. Then the introduction of phase shifts and mapping to the individual antenna elements of the interfering signal can be performed within the MATRIX in the same way as for the satellite signals.

SIGNAL RECORDING

In order to record GPS C/A-code signals in the L1 band, we use the NordNav Software GPS Receiver L1 Quad Frontend. This frontend is designed to operate with NordNav's software receiver but it also is possible to use it in a stand alone fashion for data recording. The quad frontend has a sampling rate of 16.3676 MHz in a 2 MHz 3 dB bandwidth. The data are downconverted to an intermediate frequency of 4.1304 MHz and quantized with a 2-bit analog-to-digital converter. The data then are recorded in separate but synchronous files for post-processing. The signal source is the DLR MASTER, as described in the previous section. These data files then are processed by the Stanford University GPS multi-antenna space-time adaptive software receiver. A schematic overview of the simulation setup is given in Figure 5.

We simulated a planar 2-by-2 uniform rectangular array (URA). The sensor elements are displaced by $\Delta x = \lambda / 2$ along the x-axis and by $\Delta y = \lambda / 2$ along the y-axis (λ denotes the wavelength corresponding to

the carrier frequency $f_{L1} = 1575.42$ MHz). The sensor elements are assumed isotropic. The geometry of the antenna aperture is depicted in Figure 6. We simulated a static constellation of 10 satellites transmitting GPS

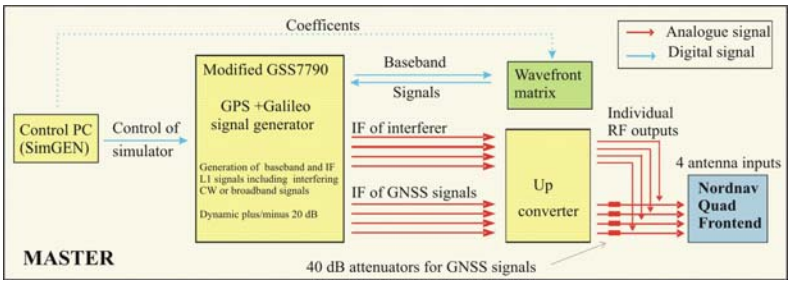

Figure 5. Schematic overview of simulation setup.

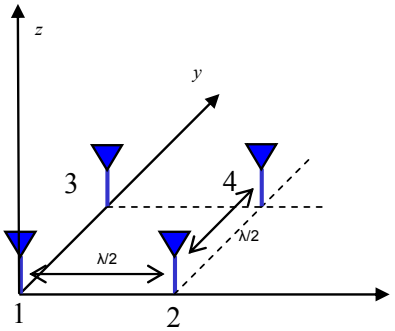

Figure 6. 2-by-2 uniform rectangular array (URA).

PRN	Azimuth	Elevation
1	0	40
2	30	30
3	60	40
4	90	50
5	120	20
6	150	60
7	210	70
8	240	20
9	270	30
10	300	80

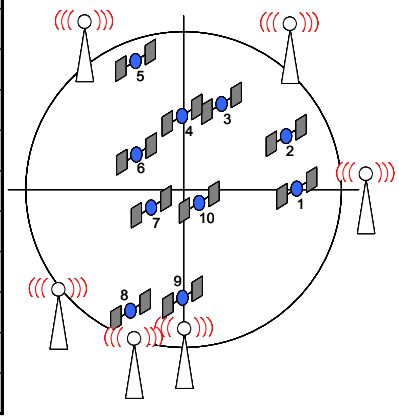

RFI	Azimuth	Elevation
1	0	0
2	45	0
3	120	0
4	225	0
5	250	0
6	270	10

Figure 7. The constellation of ten satellites as well as six near-horizon CW interferers.

C/A-code signals and six CW interferers, as depicted in Figure 7.

RESULTS

This section provides tracking results with multi-receiver test-bed hardware and space-time adaptive array processing in the software receiver. The data were processed as follows. First, the satellite signals were acquired in single-antenna FRPA mode. Then, the satellites were tracked briefly in single-antenna mode in order to refine estimates of code-phase and Doppler frequency and to capture carrier-phase in order to align to the navigation data bit boundary (allowing 20 millisecond coherent integration). Finally, after 2000 milliseconds of processing in single-antenna mode, the multi-antenna CRPA was enabled (either deterministic beamforming or adaptive beamforming and nullsteering).

The reasons for acquiring and pulling-in the signal in single-antenna mode were twofold. First, it is simpler to implement and faster computationally to perform single-antenna acquisition. Second, tracking performance is more important to characterize than acquisition performance. The reason for this is that the operational scenarios considered for this investigation have the GPS receiver tracking satellite signals and then encountering elevated levels of jamming. At that point, every effort will be spent by the receiver and STAP algorithm to maintain carrier-lock. Since acquisition requires higher C/N_0 levels than tracking, if once carrier-lock is lost, then there is no expectation of reacquiring the signal until jamming levels subside.

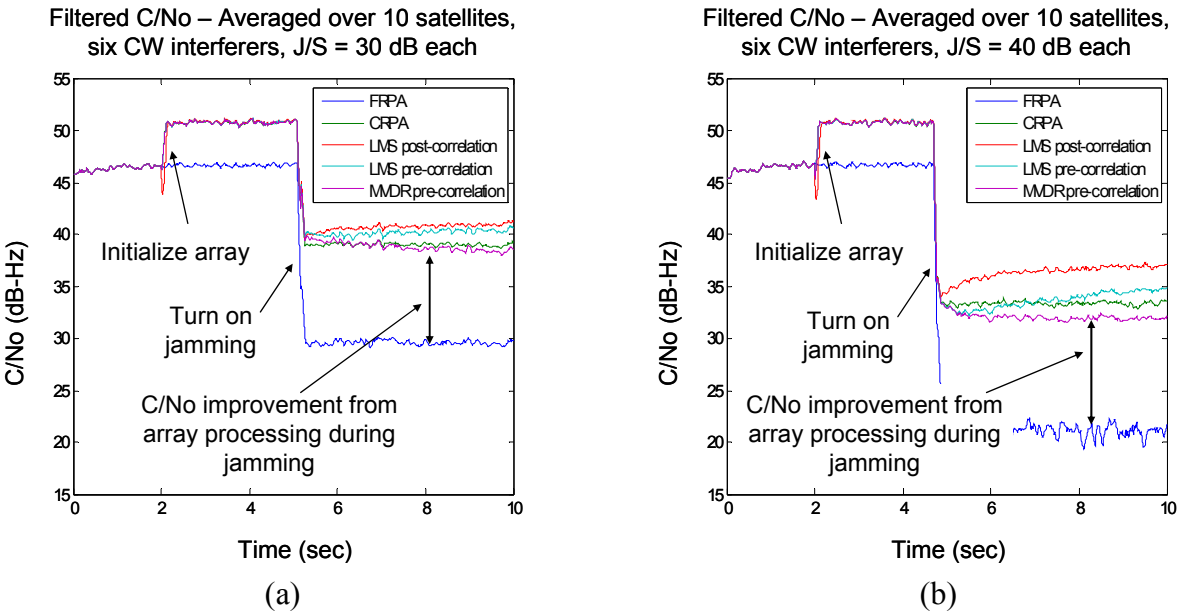

Figure 8. Processing data from Spirent simulator, DLR wavefront generator, and four-channel NordNav receiver, using Stanford University multi-antenna space-time adaptive software receiver.

LMS adaptive processing can use an initial weight vector calculated deterministically, or the weights can be initialized "blind." Blind initialization consists of setting each coefficient in the array weight vector identically to zero with the exception of the center time-tap of the master antenna element, which receives a "1" entry. For the RFI-free cases, this tracking allows estimation of the Wiener weight vector coefficients. This is important because in the absence of jamming, the LMS weight coefficients converge to the optimal Wiener values in steady-state regardless of their initial values.

Deterministic initialization of the antenna weights, whether for the beamforming CRPA or for the LMS or MVDR adaptive arrays, can be done in either of two ways: (a) by using knowledge of array geometry, satellite azimuth and elevation values, and receiver-to-receiver timing biases to compute the weight vector coefficients, or (b) by using the converged weight vector from blind initialization of LMS-based adaptive processing.

Figure 8 illustrates the average C/N_0 tracking values over a ten satellite simulated constellation. Figure 8a shows results for six jammers each at a J/S power ratio of 30 dB. Figure 8b shows results for six jammers each at a J/S power ratio of 40 dB. The blue line shows the average C/N_0 versus time for the single-antenna FRPA; the average value is approximately 47 dB-Hz. The other lines plot the average C/N_0 versus time for the 4-element deterministic CRPA, LMS-based adaptive processing with pre-correlation and post-correlation processing, and MVDR-based adaptive processing with pre-correlation processing (post-correlation processing did not produce acceptable results). For this four-antenna array in the interference-free case, the average improvement in C/N_0 is approximately 4.5 dB (this slightly underperforms the predicted value of 6 dB, and this minor degradation is due to analog hardware imperfections).

At 4000-5000 milliseconds into the tracking window, narrowband RFI illuminates the antenna array, with a J/S power ratio of 30 dB or 40 dB for each of six narrowband jammers. For the 30 dB case, the FRPA tracks at C/No of approximately 30 dB-Hz, and the various array processing methods yield approximately 40 dB-Hz. The 10 dB drop in C/No for the array processing is much less severe than the approximately 17 dB drop in C/No for the single-antenna FRPA. For the 40 dB case, the FRPA loses lock entirely. This represents a significant level of interference, and it is well beyond the capacity of this GPS receiver to maintain signal lock without special RFI processing. The antenna arrays suffer further degradation in C/No, but they all maintain signal lock with C/No in the range 32-37 dB-Hz. The reference-signal-based LMS adaptation with post-correlation beamforming performs the best of the methods surveyed here.

Table 1 shows interference rejection performance for array processing when testing with hardware in the loop (MASTER). In the interference-free case, the four-element arrays experience approximately 4 dB increase in C/No as compared to the single-element FRPA. This slightly underperforms theoretical predictions for a 4-

Table 1. C/No from hardware-in-the-loop testing, six CW RFI sources;
STAP arrays utilize spatial degrees of freedom only.

C/No (Averages over 10-satellite constellation)	Deterministic		STAP w/ 4 antennas and 1 time-tap		
	FRPA	CRPA	LMS		MVDR
			post-correlation adaptation	pre-correlation adaptation	pre-correlation adaptation
no RFI	46.6 dB-Hz	50.8 dB-Hz	50.9 dB-Hz	50.8 dB-Hz	50.8 dB-Hz
6 CW RFI emitters, 30dB J/S ratio each	29.5 dB-Hz	39.0 dB-Hz	40.9 dB-Hz	40.4 dB-Hz	38.5 dB-Hz
6 CW RFI emitters, 40dB J/S ratio each	N/A (tracking failed)	33.4 dB-Hz	36.9 dB-Hz	34.4 dB-Hz	31.9 dB-Hz

element array ($10*\log_{10}(4) = 6.0$ dB). As expected, there is no benefit to adaptive processing in the interference-free case. (Note: post-correlation MVDR processing did not perform acceptably; these results are omitted here.)

As shown in Table 1, at a J/S power ratio of 30 dB on each of the six jammers, there is a 10 dB improvement for the four-element deterministic CRPA as compared to the single-element FRPA, and a further 2 dB increase with the LMS adaptive array. The MVDR adaptive array underperforms the deterministic CRPA by 0.5 dB (averaged over the ten satellites in the constellation). This underperformance is due to channel-to-channel timing biases and receiver analog filter variation that introduce phase distortion on the received signals. At a J/S power ratio of 40 dB on each of the six jammers, the single-element FRPA loses lock entirely, and the deterministic CRPA tracks at an average C/No of 33.4 dB-Hz. Now, the LMS adaptive array (in pre-correlation mode) yields approximately 3.5 dB improvement in C/No compared to the deterministic CRPA. The MVDR adaptive array continues to underperform, now sacrificing approximately 1.5 dB compared to the deterministic CRPA.

The interference rejection results shown in Table 1 provide limited experimental verification of the predictions from simulation. The LMS adaptive algorithm was comparable in performance to simulation while the MVDR adaptive algorithm suffered from real-world analog timing effects. The reduced interference rejection performance is attributable to two key differences between simulation parameters and experimental hardware. The two differences are: (a) A/D dynamic range (2-bit converter), and (b) array spatial degrees of freedom.

LIMITATION OF EXPERIMENTAL RESULTS

The experimental set-up has demonstrated that the software receiver, in combination with operational hardware in the loop, rejects radio frequency interference. However, there are limitations to these experimental results. In particular, three unresolved issues will be discussed below.

Experimental Interference Rejection

Scenarios were created in the RF simulator with interference from six jammers. Both wideband and narrowband interference were tested, and at J/S levels up to 55 dB for narrowband and 82 dB for wideband on each of the six jammers. However, signal tracking was not successful at the higher J/S power ratios. This limitation was discovered during data analysis, and attributable to the following two reasons: (a) the 2-bit A/D had insufficient dynamic range for the higher J/S power ratios, and (b) the four-element antenna array had insufficient spatial degrees of freedom to null six widely-separated interferers.

NordNav receivers were used in the four-antenna data collection system of the hardware in the loop interference experiments. These receivers have a 2-bit A/D converter. A 2-bit A/D provides insufficient dynamic range to resolve signals at a J/S power ratio of 50 dB on each of six interference sources. For this reason, it was not possible to verify interference rejection performance at these J/S levels. Fortunately, this limitation did not

affect the experimental results at moderate interference levels. This converter limitation was not identified until after completion of the data analysis from the experimental set-up. The obvious solution is to utilize a hardware receiver with greater A/D resolution.

The high-fidelity RF signal simulator used to create signals for testing with hardware in the loop was limited by a four-receiver data collection system. The simulation portion of this investigation (reported previously [1]) utilized six interference sources, to provide maximum stress to the adaptive antenna array algorithms in a seven-element receiver. Since the hardware was limited to a four-element receiver, there were insufficient spatial degrees of freedom to adequately suppress jamming from six interference source. The obvious solution is to increase the number of data collection channels to recreate a seven-element array, or to create simulation and hardware scenarios that incorporate only three jammers.

Receiver-to-Receiver Gain Variation and Timing Biases

The multi-antenna hardware receivers were not properly synchronized, meaning that there was residual timing bias between the slave antenna channels and the master antenna. The impact of this timing bias is to require additional phase rotation in the deterministically-computed antenna weights. The remedy is to use the LMS adaptive algorithm with blind-initialization to calibrate the phase bias of each slave antenna channel. The preferred solution for an operational prototype system is improved hardware implementation.

Post-correlation MVDR

The post-correlation MVDR adaptive algorithm did not perform as expected. The LMS algorithm performed nearly equally well in both pre-correlation and post-correlation adaptation modes, while the MVDR algorithm suffered in the post-correlation mode due to excessive weight vector fluctuation. One possible cause is undetected errors in calculating the post-correlation steering vector constraint. For this reason, the results shown in this report utilize pre-correlation MVDR processing only. The resolution of this issue is left for future work.

CONCLUSION

In this work space-time adaptive processing algorithms for interference rejection in a GNSS receiver were tested under experimental conditions with recorded signals generated by a powerful hardware signal generator (MASTER). In general nearly all the assessed algorithms significantly improved the tracking performance under presence of severe RFI (six RFI sources present). The reference-signal-based LMS adaptation with post-correlation beamforming performs the best of the methods surveyed here.

The interference rejection results provide limited experimental verification of the predictions from simulation. The LMS adaptive algorithm was comparable in performance to previous simulation results while the MVDR adaptive algorithm heavily suffered from real-world analog timing effects. On the one hand a rather small A/D dynamic range (2-bit converter) and on the other hand the limited array spatial degrees of freedom provided only limited interference rejection capabilities by the space-time adaptive algorithms. Additionally, timing biases between the slave antenna channels and the master antenna, and lower gain of the slave antennas degraded the performance of the algorithms.

In order to perform further testing and a more thoroughly assessment of the performance of the presented space-time adaptive algorithms improved hardware for an operational prototype system for recording of the signals needs to be available.

ACKNOWLEDGEMENTS

The authors would like to thank Andriy Konovaltsev of DLR for his valuable contributions to this work.

References

1. D.S. De Lorenzo, J. Rife, P. Enge, and D.M. Akos, “Navigation Accuracy and Interference Rejection for an Adaptive GPS Antenna Array,” *Proc. ION GNSS 2006*, pgs. 763-773, 2006.
2. F. Antreich, O. Esbri Rodriguez, J. A. Nossek, and W. Utschick, “Estimation of Synchronization Parameters Using SAGE in a GNSS-Receiver,” *Proc. of ION GNSS 2005*, pgs. 2124-2131, 2005.
3. A. Konovaltsev, B. Belabbas, H. Denks, and A. Hornbostel, “Adaptive Antenna Against Multipath?,” *Proc. ENC-GNSS 2004*, Rotterdam, the Netherlands, 17-19 May, 2004.

4. G. Seco-Granados, J. A. Fernández-Rubio, and C. Fernández-Prades, "ML Estimator and Hybrid Beamformer for Multipath and Interference Mitigation in GNSS Receivers," *IEEE Transactions on Signal Processing*, vol. 53, no. 3, pgs. 1194-1208, 2005.
5. R.L. Fante and J.J. Vaccaro, "Cancellation of Jammers and Jammer Multipath in a GPS Receiver," *IEEE Aerospace and Electronic Systems Magazine*, vol. 13, no. 11, pgs. 25-28, 1998.
6. S.G. Carlson, C.A. Popeck, M.H. Stockmaster, and C.E. McDowell, "Rockwell Collins' Flexible Digital Anti-Jam Architecture," *Proc. ION GPS/GNSS 2003*, pgs. 1843-1851, 2003.
7. A. Hornbostel, H. Denks, and H. Venus, "First Results of Baseband Wavefront Generation with a Digital Channel Matrix for Testing of CRPA," *Proc. ION GNSS 2006*, pgs. 780-789, 2006.
8. B.D. Van Veen and K.M. Buckley, "Beamforming: A Versatile Approach to Spatial Filtering," *IEEE ASSP Magazine*, pgs. 4-24, April, 1988
9. W.F. Gabriel, "Adaptive Arrays – An Introduction," *Proc. IEEE*, vol. 64, no. 2, pgs. 239-272, 1976.
10. L.C. Godara, "Applications of Antenna Arrays to Mobile Communications, Part I: Performance Improvement, Feasibility, and System Considerations," *Proc. IEEE*, vol. 85, no. 7, pgs. 1031-1060, 1997.
11. L.C. Godara, "Applications of Antenna Arrays to Mobile Communications, Part II: Beam-Forming and Direction-of-Arrival Considerations," *Proc. IEEE*, vol. 85, no. 8, pgs 1195-1245, 1997.
12. R.T. Compton, Jr., Adaptive Antennas: Concepts and Performance, Prentice-Hall, Inc., Englewood Cliffs, N.J., 1988.
13. O.L. Frost, "An Algorithm for Linearly Constrained Adaptive Array Processing," *Proc. IEEE*, vol. 60, no. 8, pgs. 926-935, 1972.
14. S.P. Applebaum, "Adaptive Arrays," *IEEE Trans. on Antennas and Propagation*, vol. 24, no. 5, pgs. 585-598, 1976.
15. B. Widrow, P.E. Mantey, L.J. Griffiths, and B.B. Goode, "Adaptive Antenna Systems," *Proc. IEEE*, vol. 55, no. 12, pgs. 2143-2159, 1967.
16. I.F. Progri, B.W. Nicholson, D.M. Upton, and W.E. Vander Velde, "Impacts of Frequency Dependent Mutual Coupling and Channel Errors on Digital Beam Forming Antenna Performance," *Proc. ION GPS 1998*, pgs. 275-283, 1998.
17. F. Berefelt, B. Boberg, F. Eklof, J. Malmstrom, L. Paajarvi, P. Stromback, and S.L. Winkander, "INS/GPS Integration with Adaptive Beamforming," *Proc. ION GPS/GNSS 2003*, pgs. 1096-1106, 2003.
18. G.F. Hatke and T.T. Phuong, "Design and Test of a GPS Adaptive Antenna Array Processor: The Multipath Adaptive Multibeam Array (MAMBA) Processor," MIT Lincoln Laboratory Project Report GPS-16, 2004.
19. B. Widrow and S.D. Stearns, Adaptive Signal Processing, Prentice-Hall, Inc, Englewood Cliffs, N.J., 1985.